

8. Zamyatnina, V. A., Bakeeva, L. E., Aleksandrushkina, N. I. and Vanyushin, B. F., Apoptosis in etiolated wheat seedlings: 2. Effects of the antioxidant butylated hydroxytoluene and peroxides. *Russ. J. Plant Physiol.*, 2003, **50**, 251–260.
9. Vanyushin, B. F., Bakeeva, L. E., Zamyatnina, V. A. and Aleksandrushkina, N. I., Apoptosis in plants: specific features of plant apoptotic cells and effect of various factors and agents. *Int. Rev. Cytol.*, 2004, **233**, 135–179.
10. Foyer, C. H., Reactive oxygen species, oxidative signalling and the regulation of photosynthesis. *Environ. Exp. Bot.*, 2018, **154**, 134–142.
11. Aleksandrushkina, N. I., Zamyatnina, V. A., Bakeeva, L. E., Seredina, A. V., Smirnova, E. G., Yaguzhinsky, L. S. and Vanyushin, B. F., Apoptosis in wheat seedlings grown under normal day-light. *Biochem. (Mosc.)*, 2004, **69**, 285–294.
12. Batjuka, A., The impact of antimycin A on some oxidative processes and antioxidant status in the leaves of wheat seedlings (*Triticum aestivum* L.) in response to high temperature. *Agrochimica*, 2019, **63**, 109–119.
13. Kirnos, M. D., Volkova, S. A., Ganicheva, N. I., Kudryashova, I. B. and Vanyushin, B. F., Synchronous DNA synthesis in coleoptile and initial leaf of etiolated wheat seedlings: nature and ratio between nuclear and mitochondrial DNAs synthesis. *Biochem. (Mosc.)*, 1983, **148**, 1587–1595.
14. Hashimoto, H. and Possingham, J. V., Effect of light on the chloroplast division cycle and DNA synthesis in cultured leaf discs of spinach. *Plant Physiol.*, 1989, **89**, 1178–1183.
15. Givaty-Rapp, Y., Yadav, N. S., Khan, A. and Grafi, G., S1-type endonuclease 2 in dedifferentiating *Arabidopsis* protoplasts: translocation to the nucleus in senescent protoplasts is associated with de-glycosylation. *PLoS ONE*, 2017, **12**, 1–15.
16. Smirnova, T. A., Prusov, A. N., Kolomijtseva, G. Y. and Vanyushin, B. F., H1 histone in developing and aging coleoptiles of etiolated wheat seedlings. *Biochem. (Mosc.)*, 2004, **69**, 1128–1135.
17. Radha, B. N., Channakeshava, B. C., Bhanuprakash, K., Gowda, K. T., Ramachandrappa, B. K. and Munirajappa, R., DNA damage during seed ageing. *J. Agric. Vet. Sci.*, 2014, **7**, 34–39.
18. Hameed, A., Iqbal, N. and Malik, S. A., Effect of D-mannose on antioxidant defence and oxidative processes in etiolated wheat coleoptiles. *Acta Physiol. Plant.*, 2014, **36**, 161–167.
19. Latrasse, D., Benhamed, M., Bergounioux, C., Raynaud, C. and Delarue, M., Plant programmed cell death from a chromatin point of view. *J. Exp. Bot.*, 2016, **67**, 5857–5900.
20. Bakeeva, L. E., Zamyatnina, V. A., Shorning, B. Y., Aleksandrushkina, N. I. and Vanyushin, B. F., Effect of the antioxidant ionol (BHT) on growth and development of etiolated wheat seedlings: control of apoptosis, cell division, organelle ultrastructure, and plastid differentiation. *Biochem. (Mosc.)*, 2001, **66**, 850–859.
21. Wakiuchi, N., Mukai, N., Kubo, S., Oji, Y. and Shiga, H., Changes in DNA level of growing barley seedlings. *Soil Sci. Plant Nutr.*, 1990, **36**, 469–473.
22. Nordzieke, D. E. and Medraño-Fernandez, I., The plasma membrane: a platform for intra- and intercellular redox signalling. *Antioxidants*, 2018, **7**, 1–34.
23. Takele, A., Differential responses of electrolyte leakage and pigment compositions in maize and sorghum after exposure to and recovery from pre- and post-flowering dehydration. *Agric. Sci. China*, 2010, **9**, 813–824.
24. Rolny, N., Costa, L., Carrión, C. and Guiamet, J. J., Is the electrolyte leakage assay an unequivocal test of membrane deterioration during leaf senescence? *Plant Physiol. Bioch.*, 2011, **49**, 1220–1227.
25. Ali, M. K., Azhar, A. and Galani, S., Response of rice (*Oryza sativa* L.) under elevated temperature at early growth stage: physiological markers. *Russ. J.*, 2013, **8**, 11–19.
26. Iakimova, E. T. and Woltering, E. J., The wound response in fresh-cut lettuce involves programmed cell death events. *Protoplasma*, 2018, **255**, 1225–1238.
27. Batjuka, A. and Škute, N., Evaluation of superoxide anion level and membrane permeability in the functionally different organs of *Triticum aestivum* L. exposed to high temperature and antimycin A. *Curr. Sci.*, 2019, **117**, 440–447.
28. Batjuka, A. and Škute, N., The effect of antimycin A on the intensity of oxidative stress, the level of lipid peroxidation and antioxidant enzyme activities in different organs of wheat (*Triticum aestivum* L.) seedlings subjected to high temperature. *Arch. Biol. Sci.*, 2017, **69**, 743–752.

Received 19 November 2020; revised accepted 24 November 2021

doi: 10.18520/cs/v122/i1/93-98

## A balloon-borne experiment for quasi-Lagrangian frame of reference measurements of intrinsic frequency spectrum of gravity waves in the stratosphere

Karanam Kishore Kumar<sup>1,\*</sup>,  
 K. V. Subrahmanyam<sup>1</sup>, B. Suneel Kumar<sup>2</sup>,  
 K. V. Suneeth<sup>3</sup>, M. Pramitha<sup>1</sup>, N. Koushik<sup>1</sup>,  
 N. Nagedra<sup>2</sup> and G. Stalin Peter<sup>2</sup>

<sup>1</sup>Space Physics Laboratory, Vikram Sarabhai Space Centre, Thiruvananthapuram 695 022, India

<sup>2</sup>Tata Institute of Fundamental Research Balloon Facility, Hyderabad 500 062, India

<sup>3</sup>India Meteorology Department, New Delhi 110 003, India

In the present communication, first results from an experiment to measure intrinsic frequency spectrum of atmospheric gravity waves using balloon-borne quasi-Lagrangian frame of reference observations in the mid-stratosphere over a tropical station, Hyderabad (17.4°N, 78.2°E) are discussed. A zero-pressure polyethylene balloon with GPS-sonde payload was drifted at ~31 km altitude for a horizontal distance of ~100 km for measuring pressure, wind and temperature at 1 sec temporal resolution. The measured altitude of the balloon showed variability within ±100 m, thus ensuring a near horizontal drift. These observations are used to estimate the intrinsic frequency spectrum of gravity waves in the mid-stratosphere over an Indian observational site. The successful experiment has opened up a new avenue for studying not only the stratospheric gravity wave dynamics, but also for exploring the horizontal mapping of stratospheric trace gases.

**Keywords:** Balloon-borne experiment, gravity waves, intrinsic frequency spectrum, stratosphere, trace gases.

\*For correspondence. (e-mail: kishore\_nmrf@yahoo.com)

ATMOSPHERIC gravity waves, also known as buoyancy waves, are one of the ubiquitous phenomena in the earth's atmosphere. Excited in the lower atmosphere, these waves propagate vertically up and have profound impact on the structure and dynamics of the middle and upper atmosphere<sup>1,2</sup>. These waves vertically couple the various layers of the earth's atmosphere by transporting energy and momentum. The mean flow acceleration imparted by these waves is one of the contributors in driving the long-period atmospheric oscillations such as the quasi-biennial oscillation and semi-annual oscillation in the equatorial middle atmosphere<sup>2–4</sup>. The main sources of gravity waves are orographical features, atmospheric convection, wind shears, frontal systems, jet streams and other secondary generative mechanisms like breaking of tides/planetary waves and general instabilities that can exist at all heights in the atmosphere<sup>1,5,6</sup>. One of the intriguing aspects of the atmospheric gravity waves is their universal frequency and wavenumber spectra<sup>7</sup>. It has been noted that the wavenumber and frequency spectra of gravity wave-induced perturbations in geophysical parameters exhibit similar characteristics in the saturated regime, irrespective of the time of observation or geographical location over which it is measured.

Several observation techniques are widely employed for the study of gravity waves, such as rocket sounding<sup>8</sup>, aircraft/balloon measurements<sup>9–11</sup>, radar<sup>3,12</sup>, lidar<sup>13</sup>, and satellite observations<sup>4,14</sup>. Most of these observations, except aircraft, provide the vertical wavenumber as well as frequency spectra. On the other hand, aircraft measurements provide horizontal wavenumber spectra of gravity waves, which are limited to the troposphere. Majority of these ground- and space-based observations provide Doppler-shifted frequency of the gravity waves rather than their intrinsic frequency. These two frequencies are related by the following equation

$$\omega_i = \omega_D - U k,$$

where  $\omega_i$  is the intrinsic frequency,  $\omega_D$  the Doppler-shifted frequency,  $U$  the wind in the direction of wave propagation and  $k$  is the horizontal wavenumber. The frequency that would be observed in a frame of reference moving with the horizontal background wind is the intrinsic frequency and is one of the important parameters in gravity-wave studies. However, it is difficult to measure the intrinsic frequency of the gravity waves directly in the middle atmosphere using conventional measurement techniques such as vertical balloon sounding, radar and lidar. In most studies this parameter is indirectly inferred from theoretical assumptions. Hertzog and Vial<sup>15</sup> studied the intrinsic frequency spectra of gravity waves using superpressure balloons (SPBs). They employed ultra-long-duration balloons over the equatorial region to characterize the gravity waves with special emphasis on momentum fluxes. Recently, in an effort to provide worldwide internet

coverage under Project Loon, several SPBs were launched continuously in the lower stratosphere. They measure wind, temperature and pressure with very high temporal and spatial resolution, which is useful for characterizing the intrinsic spectra of gravity waves<sup>10</sup>.

Though there are several observations of gravity waves right from the troposphere to the thermosphere over the Indian region, to the best of our knowledge, there have been no attempts in the past to measure the intrinsic frequency spectrum in any part of the atmosphere. In view of this an experiment was designed and carried out by drifting a zero-pressure polyethylene (ZP) balloon along with a GPS sonde in the horizontal direction in the stratosphere at ~31 km to measure wind, temperature and pressure for about 100 km distance from the Tata Institute of Fundamental Research-Balloon Facility (TIFR-BF) at Hyderabad. To the best of our knowledge, such experiments to study the high-frequency atmospheric gravity waves over the Indian region have not been conducted earlier. However, Appu *et al.*<sup>16</sup> carried out an experiment by horizontally drifting a balloon at 900 hPa (~1 km altitude) to study the spatial distribution of meteorological parameters over the Arabian Sea and Indian Ocean region. An Indo-French joint scientific team released a total of 17 constant-altitude balloons to study the transportation of aerosols and trace gases. This experiment was limited to atmospheric boundary-layer measurements, whereas the present experiment focuses on the lower stratospheric measurements.

Figure 1 *a* shows a photograph depicting the preparation of a balloon launching on 13 September 2019 from TIFR-BF. The balloon was launched around 00:26 (IST) with a team of experts at the Balloon Facility and its horizontal drifting was started at around 31 km altitude. Figure 1 *b* shows the track of the balloon derived from GPS coordinates. It depicts the vertical ascent, horizontal drift and descent of the balloon as a function of longitude, latitude and altitude. The horizontal drift of the balloon was about 100 km at 31 km altitude. Though there was scope for drifting of the balloon for a larger distance, it was restricted to 100 km considering the recovery of flight-control instrumentation after the experiment. Given the high wind speed at 31 km altitude, it will be difficult to recover the flight-control instrumentation and thus the experiment was terminated at a preset time. With this experimental set-up, the drifting of the balloon was perfectly achieved in the mid-stratosphere. Figure 1 *c* shows the vertical profile of temperature in the troposphere and stratosphere up to 31 km altitude, after which horizontal drifting started. One can notice the oscillatory nature of the temperature field in the stratosphere owing to the propagation of atmospheric waves. The cold-point tropopause altitude was found to be around 18.5 km in this profile. Figure 1 *d* shows the vertical profile of zonal and meridional winds derived from the rate of change of position of the balloon. The vertical profile of zonal winds shows

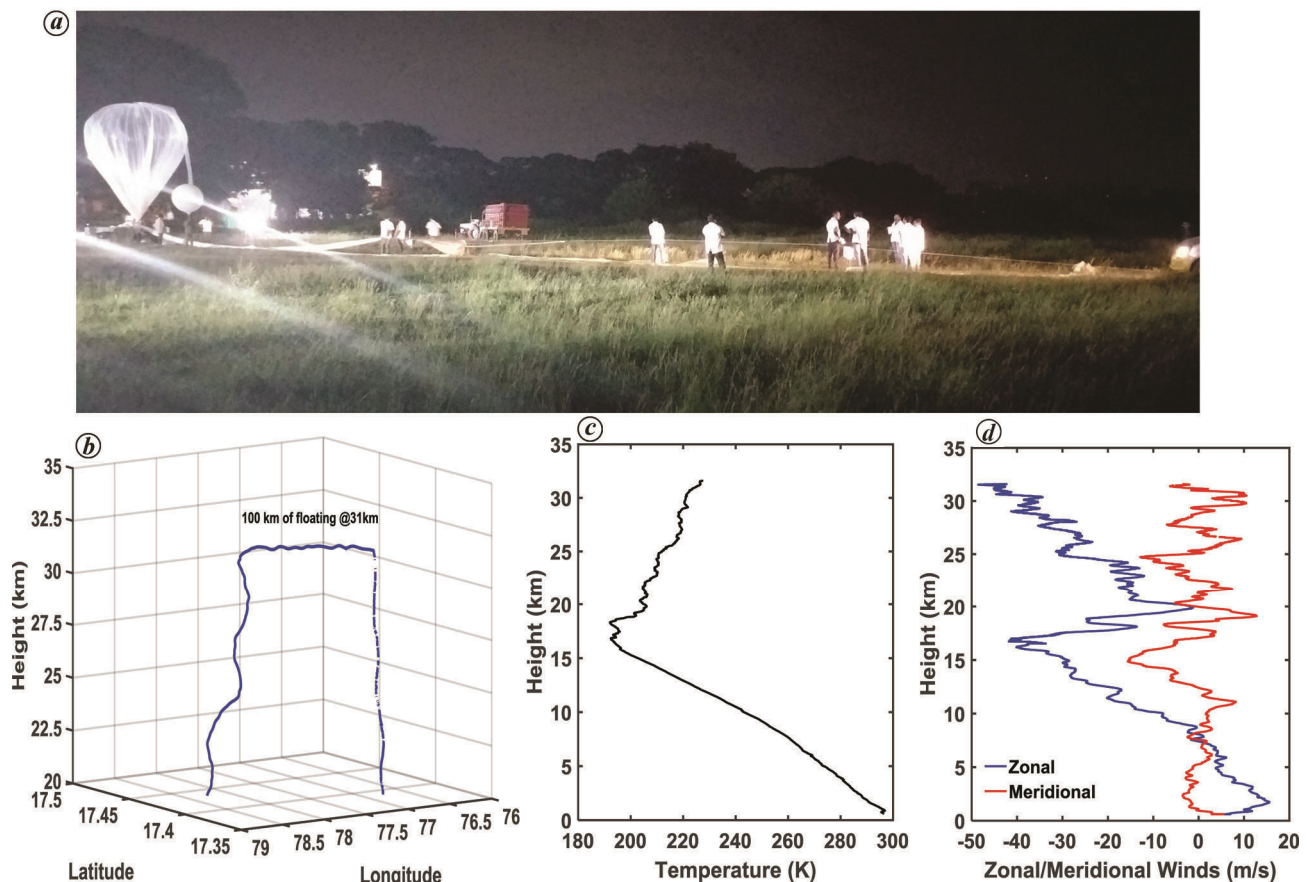


**Figure 1.** *a*, Photograph depicting preparation for the balloon experiment at the TIFR Balloon Facility in Hyderabad. *b*, Path of the balloon retrieved from the GPS receiver. *c*, Vertical profile of temperature. *d*, Vertical profiles of zonal and meridional winds on 13 September 2019.

the signature of tropical easterly jet (TEJ) at 16.5 km altitude with peak magnitude of  $42 \text{ ms}^{-1}$ . The zonal wind profile also shows large westward winds of the order of  $-50 \text{ ms}^{-1}$  at 31 km altitude, where the balloon started its horizontal drifting. On the other hand, meridional winds are benign throughout the troposphere and stratosphere with magnitudes within  $\pm 15 \text{ ms}^{-1}$ . The meridional wind profile exhibits a wave-like structure, especially in the stratosphere.

Figure 2 shows the various parameters measured during the horizontal drift of the balloon. These measurements are useful in estimating the intrinsic frequency spectra of gravity waves, as discussed earlier. Figure 2 *a* shows the altitudinal variation of the balloon during the horizontal drift. It is interesting to note that the deviation of the balloon from the mean altitude (31.6 km) was within  $\pm 100 \text{ m}$ . To be precise, the altitude variation was within  $\pm 50 \text{ m}$  for most parts of the drift. This particular observation confirms the horizontal drifting of the balloon and thus the success of the experiment. Figure 2 *b* and *c* shows the pressure and temperature variations along the balloon path. The pressure perturbations were within  $\pm 0.15 \text{ hPa}$  and those of temperature within  $\pm 5 \text{ K}$ . Though the stratosphere is stable, significant horizontal tempera-

ture perturbations were observed due to the propagation of atmospheric waves. The temperature perturbations caused by these waves drive the stratosphere away from the radiative equilibrium. Figure 2 *d* and *e* shows the zonal and meridional winds along the balloon path. Zonal winds as strong as  $45 \text{ ms}^{-1}$  were observed during the experiment whereas meridional winds of the order of  $5 \text{ ms}^{-1}$  were observed at the balloon floating altitude.

The main objective of the experiment was to demonstrate the capability for horizontal drifting of the balloon and to estimate the intrinsic frequency of the gravity wave spectrum. The measurements made by the drifting balloon are in the frame of reference of disturbance. The observations depicted in Figure 2 span for  $\sim 32 \text{ min}$  and thus only high-frequency part of the spectra can be estimated using these measurements. In fact, one should have long-duration measurements to completely estimate the gravity wave intrinsic frequency spectrum right from inertial frequency to Brunt–Väisälä frequency (BVF). Figure 3 shows the estimated intrinsic frequency spectra of the measured geophysical parameters. The mean removed perturbations were subjected to Fourier analysis to estimate these spectra. Figure 3 *a* shows the intrinsic frequency spectra of zonal and meridional winds. The zonal

winds show a peak at 0.0013 cycles/sec (~12.6 min period), whereas the meridional wind spectrum shows a peak at 0.0022 cycles/sec (~7.5 min) corresponding to BVF. The zonal wind spectrum also shows a broad peak at BVF ranging from 0.0022 to 0.0035 cycles/sec. Figure 3 *b* depicts the intrinsic frequency spectra of pressure and vertical displacement of the balloon. A striking feature of these two spectra is the prominent peak at BVF. It is known that BVF is a vertical oscillation and will be prominently seen in the vertical velocity as well as related parameters. Pressure and vertical displacement being closely related with the vertical velocity, BVF is prominently observed in these two parameters. This particular feature vouches for the successful measurements of spatially varying geo-physical parameters at a given altitude by horizontal drifting of the balloon. Figure 3 *c* shows the intrinsic frequency spectrum of temperature perturbations. The temperature perturbations were normalized with the mean temperature before Fourier analysis. This spectrum also shows a broad peak at ~0.0022 cycles/sec corresponding to BVF. The BVF values inferred from each spectrum

shown in Figure 3 are displayed in Table 1, which also shows the mean BVF in the 25–30 km altitude estimated from the vertical profile of temperature shown in Figure 1 *b*, as well as a typical value for the tropical stratosphere in the same height range. There are slight differences in the estimated BVF from the temperature profile and those inferred from the spectra. This can be attributed to some extent to frequency resolution of the spectrum. It is also to be noted that the BVF estimated from temperature profile is a point observation, whereas the spectrum is estimated using observations spreading over ~100 km. The BVF estimated using frequency spectra is lower than the typical values reported in the literature. This will have implications while estimating the saturation amplitudes of gravity waves as well as their momentum fluxes using polarization relation in numerical models as well as observations. However, the BVF values estimated from spectra are instantaneous, whereas typical values are from climatology. The intrinsic frequency spectrum of temperature can be used to estimate the gravity wave momentum fluxes, which is one of the important parameters to quantify the gravity wave impact on background winds. In principle, gravity wave momentum flux ( $u'w'$ ) can be estimated directly if gravity wave perturbations in horizontal ( $u'$ ) and vertical ( $w'$ ) winds are known. However, vertical wind observations at gravity-wave scales are not possible in the stratosphere. The only instrument that can measure vertical velocities of clear air is the VHF radar and its measurements are limited to 22 km altitude in the lower stratosphere. In the absence of direct vertical velocity measurements, one can apply the gravity-wave polarization relation and derive an expression for their momentum fluxes. This formulation requires knowledge of intrinsic frequency, which is difficult to measure using ground-based measurements as the observed frequencies will be Doppler-shifted. Using the present experiment with relatively longer duration, we can measure the intrinsic frequency spectra which can be directly employed to estimate the gravity-wave momentum fluxes. Atmospheric gravity waves being a sub-grid-scale process are parameterized in the numerical models. In a typical parameterization scheme, a source spectrum of gravity waves with specified

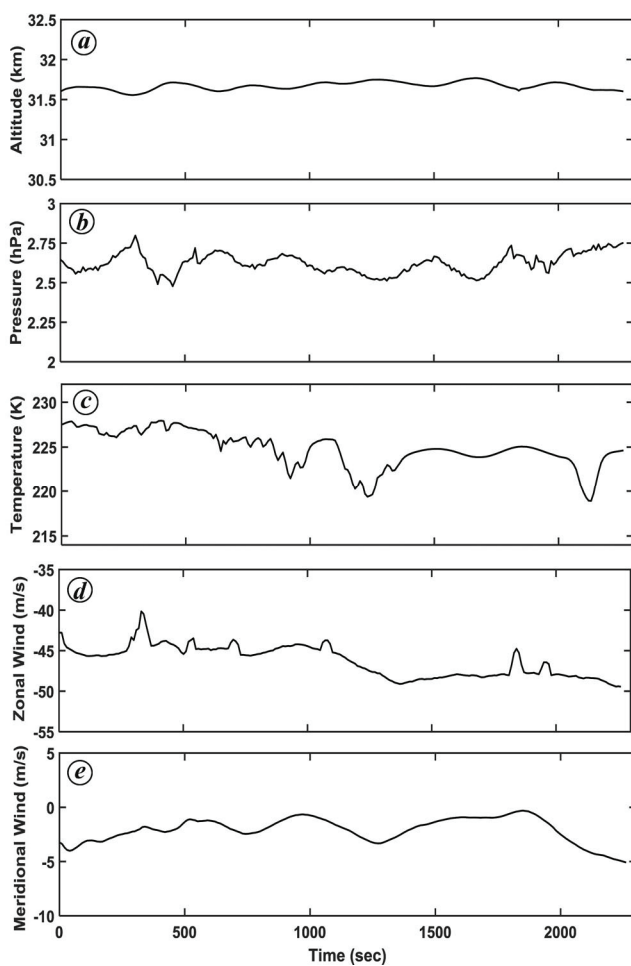


**Figure 2.** Time series of (a) altitude of the balloon, (b) pressure, (c) temperature, (d) zonal wind and (e) meridional wind measured during horizontal drifting on 13 September 2019.

**Table 1.** Brunt–Väisälä frequency (BVF) estimated from the spectra depicted in Figure 3

Parameter	BVF derived from the spectrum (cycles/sec)
Zonal wind	0.0026
Meridional wind	0.0022
Temperature	0.0022
Pressure	0.0026
Displacement	0.0026

Mean (25–30 km) BVF estimated from temperature profile: 0.0035 (cycles/sec).

Typical BVF observed in the tropical stratosphere: 0.0032 (cycles/sec).

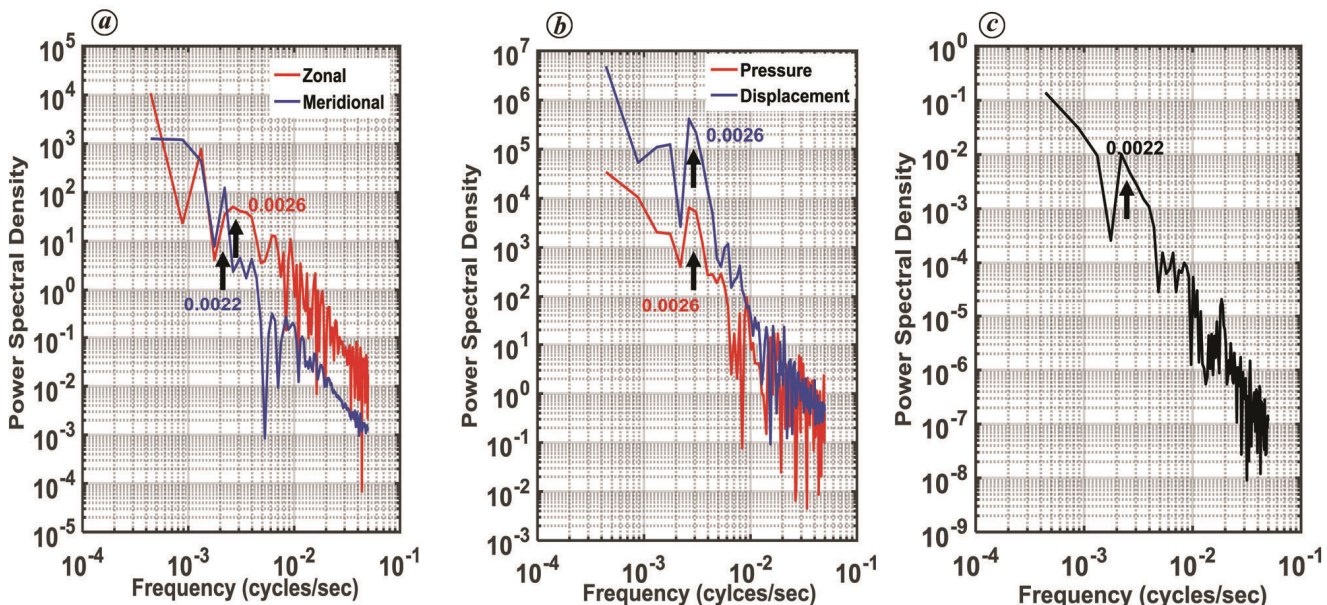


**Figure 3.** Intrinsic frequency spectrum of (a) zonal and meridional wind perturbations, (b) vertical displacement and pressure, and (c) normalized temperature perturbations on 13 September 2019. Black arrows indicate peaks corresponding to Brunt–Väisälä frequency and numerical values provide the corresponding magnitudes (cycles/sec).

amplitudes as a function of phase speeds is assumed, and the same is propagated from the upper troposphere to the middle atmosphere with complete physics of gravity-wave propagation. At each height interval ( $\sim 1$  km), the gravity-wave momentum flux is estimated after verifying wave-breaking and saturation. If parameterization schemes provide anomalous gravity-wave momentum fluxes, based on the observational statistics, these fluxes can be constrained. Thus by estimating the gravity-wave momentum fluxes one can constrain the parameterization schemes. The results discussed here are preliminary in nature and long-duration balloon measurements are needed to completely characterize the gravity-wave spectrum right from inertial frequency to BVF.

The important result from the present study is the demonstration of horizontal drifting of the balloon at TIFR-BF. With this successful flight, it is planned to carry out a campaign with long-duration balloon flights and additional payloads along with a communication module to upload data to a geostationary satellite. A preliminary survey to carry out the long-duration balloon experiment over the Indian region has been done. It was found that releasing a balloon over the Andaman and Nicobar Islands, horizontally drifting the balloon in the mid-stratosphere during the westward phase of the quasi-biennial oscillation and then collecting the payload over southern India can provide measurements up to  $\sim 1500$  km. Such experiments can provide additional information on stratospheric gravity waves in the quasi-Lagrangian frame of reference, which in turn is useful in constraining the gravity-wave parameterization schemes in numerical models, as discussed earlier.

1. Fritts, D. C. and Alexander, M. J., Gravity wave dynamics and effects in the middle atmosphere. *Rev. Geophys.*, 2003, **41**(1), 1003; <https://doi.org/10.1029/2001RG000106>.
2. Holton, J. R., The role of gravity wave induced drag and diffusion in the momentum budget of the mesosphere. *J. Atmos. Sci.*, 1982, **39**(4), 791–799; [https://doi.org/10.1175/15200469\(1982\)039<0791:TROGWI>2.0.CO;2](https://doi.org/10.1175/15200469(1982)039<0791:TROGWI>2.0.CO;2)
3. Antonita, T. M., Ramkumar, G., Kumar, K. K. and Deepa, V., Meteor wind radar observations of gravity wave momentum fluxes and their forcing toward the mesospheric semi-annual oscillation. *J. Geophys. Res.*, 2008, **113**, D10115; <https://doi.org/10.1029/2007JD009089>.
4. John, S. R. and Kumar, K. K., TIMED/SABER observations of global gravity wave climatology and their interannual variability from stratosphere to mesosphere lower thermosphere. *Clim. Dyn.*, 2012, **39**(6), 1489–1505; <https://doi.org/10.1007/s00382-012-1329-9>.
5. Fovell, R., Durran, D. and Holton, J. R., Numerical simulations of convectively generated stratospheric gravity waves. *J. Atmos. Sci.*, 1992, **49**, 1427–1442.
6. Alexander, M. J., Holton, J. R. and Durran, D. R., The gravity wave response above deep convection in a squall line simulation. *J. Atmos. Sci.*, 1995, **52**, 2212–2226.
7. Van Zandt, T. E., A universal spectrum of buoyancy waves in the atmosphere. *Geophys. Res. Lett.*, 1982, **9**, 575–578.
8. Rapp, M., Strelkinov, B., Müllermann, A., Lübken, F. J. and Fritts, D. C., Turbulence measurements and implications for gravity wave dissipation during the MaCWave/MIDAS rocket program. *Geophys. Res. Lett.*, 2004, **31**, L24S07; <https://doi.org/10.1029/2003GL019325>.
9. Zhang, F., Wei, J., Zhang, M., Bowman, K. P., Pan, L. L., Atlas, E. and Wofsy, S. C., Aircraft measurements of gravity waves in the upper troposphere and lower stratosphere during the START08 field experiment. *Atmos. Chem. Phys.*, 2015, **15**, 7667–7684.
10. Schoeberl, M. R., Jensen, E., Podglajen, A., Coy, L., Lodha, C., Candido, S. and Carver, R., Gravity wave spectra in the lower stratosphere diagnosed from project loon balloon trajectories. *J. Geophys. Res.: Atmos.*, 2017, **122**, 8517–8524; doi:10.1002/2017JD026471.

11. Pramitha, M., Kishore Kumar, K. and Venkat Ratnam, M., Observations and model predictions of vertical wavenumber spectra of gravity waves in the troposphere and lower stratosphere over a tropical station. *J. Atmos. Sol. Terr. Phys.*, 2021, **216**, 105601.
12. Vincent, R. A. and Reid, I. M., HF Doppler measurements of mesospheric momentum fluxes. *J. Atmos. Sci.*, 1983, **40**(5), 1321–1333; [https://doi.org/10.1175/15200469\(1983\)040<1321:HDMOMG>2.0.CO;2](https://doi.org/10.1175/15200469(1983)040<1321:HDMOMG>2.0.CO;2)
13. Ramkumar, G. *et al.*, Seasonal variation of gravity waves in the Equatorial Middle Atmosphere: results from ISRO's Middle Atmospheric Dynamics (MIDAS) program. *Ann. Geophys.*, 2006, **24**, 2471–2480; doi:10.5194/angeo-24-2471-2006.
14. Preusse, P. *et al.*, Space-based measurements of stratospheric mountain waves by CRISTA. 1. Sensitivity, analysis method, and a case study. *J. Geophys. Res.*, 2002, **107**(D23), 8178; <https://doi.org/10.1029/2001JD000699>.
15. Hertzog, A. and Vial, F., A study of the dynamics of the equatorial lower stratosphere by use of ultra-long-duration balloons: 2. Gravity waves. *J. Geophys. Res.*, 2001, **106**, 22745–22761.
16. Appu, K. S. *et al.*, Spatial distribution of meteorological parameters around 900 hPa level over the Arabian Sea and Indian Ocean regions during the IFP-99 of the INDOEX programme as revealed from the constant altitude balloon experiments conducted from Goa. *Curr. Sci.*, 2001, **80**, 89–96.

**ACKNOWLEDGEMENTS.** We thank Tata Institute of Fundamental Research-Balloon Facility members for their expertise and cooperation in carrying out this special experiment. We also thank Dr Radhika Ramachandran (former Director, Space Physics Laboratory, Vikram Sarabhai Space Centre) for encouragement and support while carrying out this experiment.

Received 12 October 2021; revised accepted 22 November 2021

doi: 10.18520/cs/v122/i1/98-103